Head and Neck Pathol (2017) 11:419–426
DOI 10.1007/s12105-017-0784-3

ORIGINAL PAPER

Ultrastructural Characterization of Mammary Analogue Secretory Carcinoma of the Salivary Glands: A Distinct Entity from Acinic Cell Carcinoma?

Julie Guilmette[1,4] · Gunnlaugur P. Nielsen[2,3] · William C. Faquin[2,3,5] · Martin Selig[2,3] · Vânia Nosé[2,3] · Anthony W. S. Chi[2,3] · Peter M. Sadow[2,3,5]

Received: 2 December 2016 / Accepted: 30 January 2017 / Published online: 13 February 2017

Abstract Mammary analogue secretory carcinoma (MASC) of the salivary glands is a recently described neoplasm of the salivary glands with a characteristic morphology complemented by a specific cytogenetic translocation and gene rearrangements. Although immunophenotypic and cytogenetic differences allow for a more reliable distinction, ultrastructural features can also provide important information about the relationship between MASC, classic acinic cell carcinoma (AciCC), and AciCC intercalated duct cell-predominant variant. Following approval from the hospital's institutional review board, 7 cases of MASC, 8 cases of classic AciCC, and 4 cases of AciCC intercalated duct cell-predominant variant were retrieved from the pathology files of Massachusetts General Hospital from 2012 to 2015. Electron microscopy was performed using formalin-fixed, paraffin-embedded tissue. Ultrastructural features of all 19 neoplasms of the salivary glands were recorded. The predominant cell-types observed in MASC are those with intercalated/striated duct cell differentiation. These features include prominent invaginations of the cell surface studded with microvilli, and some intra- and intercellular lumina also with a microvillous surface. Classic AciCC dominant cell-type recapitulates acinar cell differentiation. These cells contain large intracytoplasmic zymogen-like granules. AciCC intercalated duct cell-predominant variant showed both cell populations in various proportions with the intercalated/striated duct cell type usually being the dominant one. MASC presents with distinctive ultrastructural features that allows its proper differentiation from classic AciCC. However, significant ultrastructural features overlaps between both AciCC intercalated duct cells-predominant and classic AciCC and MASC. These findings indicate a very close proximity between these tumors.

Keywords Mammary analogue secretory carcinoma · Salivary gland tumor · Electron microscopy · Acinic cell carcinoma

Introduction

Mammary analogue secretory carcinoma (MASC) is a recently described neoplasm of the salivary glands that harbors a distinct immunohistochemical profile and a specific cytogenetic translocation (12; 15) (q13; q25) resulting in an *ETV6-NTRK3* gene rearrangement [1–10], in addition to other recently described *ETV6* partners [4, 11]. Until this unique ancillary profile was reported, MASC was previously considered to be an acinic cell carcinoma (AciCC) "zymogen poor" or intercalated duct-cell predominant variant [5–8, 12, 13].

Electron microscopy (EM) plays an essential role in identifying key features used to characterize and diagnose tumors, which sometimes cannot be achieved solely with conventional light microscopy. In addition, EM has

✉ Peter M. Sadow
psadow@mgh.harvard.edu

1 Department of Pathology, University of Montreal Hospital Center, Montreal, QC, Canada

2 Pathology Service, Massachusetts General Hospital, Harvard Medical School, Boston, MA, USA

3 Department of Pathology, Massachusetts General Hospital, 55 Fruit Street, Boston, MA 02114-2696, USA

4 Department of Pathology and Molecular Biology, N-528 Faculté de Médecine, Université de Montréal, 2900 Boulevard Edouard-Montpetit, Montreal, QC H3C 3J7, Canada

5 Department of Otolaryngology, Massachusetts Eye and Ear Infirmary, Boston, MA 02114, USA

provided insight on neoplastic cellular differentiation and cellular origins found in common tumors of the salivary glands as the latter were compared to normal ultrastructural histology of the salivary glands [14, 15].

Although immunophenotypic and cytogenetic profiles are diagnostically very useful, ultrastructural features of MASC can provide important information about the relationship between MASC and AciCC, while identifying characteristic features that would contribute to making the correct diagnosis.

Materials and Methods

Following approval from the institution review board (IRB# 2013P001818), 7 cases of MASC, 8 cases of classic AciCC, and 4 cases of AciCC intercalated duct cell-predominant were retrieved from the pathology files of the Massachusetts General Hospital from 2012 to 2015. Hematoxylin and eosin stained (H/E) slides including ancillary studies and cytogenetic reports ordered at the time of initial diagnosis were reviewed. *ETV6* fluorescence in situ hybridization (FISH) using a break-apart *ETV6* probe (Abbot Molecular, Des Plains, IL) was performed on all MASC to confirm rearrangement of *ETV6* at 12p13. In addition, *ETV6* FISH was also performed on all 4 cases of AciCC intercalated duct cells-predominant variant to avoid possible cross contamination with MASC. EM was performed using formalin-fixed, paraffin-embedded tissue. Corresponding H/E slides were matched to the paraffin blocks and representative areas containing only tumor tissue were cut out using a razor blade. All selected tissue samples were processed using a standard protocol. Tissue samples were placed in xylene overnight and rehydrated in a series of 1-h aqueous ethanol dilutions and fixed with glutaraldehyde. One-micron sections were cut with an LKB 8801 ultramicrotome and diamond knife, stained with lead citrate, and examined with a Phillips 301 transmission electron microscope. All cases were analyzed by two experienced electron microscopists (MKS, GPN). Images were captured with an Advanced Microscopy Techniques (AMT) digital CCD camera. Ultrastructural features of MASC were compared to those of classic AciCC and its variant intercalated duct cell-predominant.

Results

Seven cases of MASC were identified, which includes 2 males and 5 females with a mean age of 45 years, ranging from range 33–67 years (Table 1). Six of them are located in the parotid gland and one in the buccal mucosa. The recorded tumor size is quite variable and ranges from 0.6 to 4.0 cm in the largest diameter (mean of 2.3 cm). For all cases, the tumor cells show a strong and diffuse staining pattern for both S100 protein and mammaglobin [5, 7]. At the time of initial diagnosis, most tumors were well-circumscribed within the salivary gland with the exception of one tumor, which showed neoplastic extension into the surrounding skeletal muscle, in addition to lymphovascular invasion (case 3). Another case showed lymphovascular invasion without extraglandular extension (case 4). Otherwise, there was no perineural invasion or metastasis reported among these selected cases.

Among the 8 cases of classic AciCC, 1 male and 7 females were identified ranging from 25 to 77 years old (mean of 57 years) (Table 1). Six of the tumors were located in the parotid gland and two were located in the parapharyngeal region. The recorded tumor size was variable and ranged from 1.0 to 3.1 cm (mean of 2.2 cm). The size of one tumor was not recorded as only the biopsy specimen was available (case 8). The diagnosis of classic AciCC was made on combined features of both morphology and immunohistochemistry. When documented, most classic AciCC were confined to the salivary gland and did not show features of lymphovascular or perineural invasion, with the exception of one case (case 6).

Four cases of AciCC intercalated duct cell-predominant variant were identified (Table 1), which included 3 males and 1 female ranging from 22 to 77 years of age (mean of 54 years). The size of the tumor varied from 1.4 to 3.5 cm in their largest diameter (mean of 2.5 cm). All tumors were confined to the parotid gland. When documented, there was no evidence of lymphovascular invasion, perineural invasion, or lymph node metastases. The diagnosis of AciCC intercalated duct cell-predominant variant was made using both combined features of histology and immunohistochemistry. FISH analysis to assess for *ETV6* gene rearrangement at 12p13 was performed on all cases to avoid cross contamination with MASC. All four cases were negative for *ETV6* rearrangement.

Electronic Microscopy

Ultrastructural examination of MASC revealed three cell populations. The dominant cell-type features flattened to cuboidal cells with inter- and intracellular lumina studded with numerous microvilli (Fig. 1a, b). Some of these cells contained cytoplasm filled with many small secretory-like granules. Exocytosis of secretory-like granules is identified in one case (Fig. 1c). These cells are often organized around a centered lumen filled with electron-dense bubbly material recapitulating a microcystic/ductal pattern, well-known in MASC. Based on documented ultrastructural features of normal salivary gland, this dominant cell-type

Table 1 Clinicopathologic findings of patients with MASC, Classic AciCC and AciCC Intercalated Duct Cell-Predominant Variant

Tumor / Case no.	Age (yr)	Sex	Tumor location	Tumor size (cm)	Tumor extension	FISH
MASC						
Case 1	55	M	Left parotid	3.5	No LN mets No LVI No PNI	ETV6 rearrangement
Case 2	33	F	Left parotid	2.4	No LN mets No LVI No PNI	ETV6 rearrangement
Case 3	42	M	Left parotid	2.9	LVI+ Extend into MSK No PNI No LN mets	ETV6 rearrangement
Case 4	64	F	Right buccal gland	0.6	LVI + No PNI No LN mets	ETV6 rearrangement
Case 5	45	F	Left parotid	1.8	No LVI No PNI	ETV6 rearrangement
Case 6	34	F	Left parotid	4.0	No LVI No PNI No LN mets	ETV6 rearrangement
Case 7	44	F	Left parotid	1.1	No LVI No PNI	ETV6 rearrangement
Classic AciCC						
Case 1	50	F	Left parotid	2.3	No PNI	N/P
Case 2	64	F	Right parotid	2.2	No PNI No LVI No LN mets	N/P
Case 3	55	F	parapharyngeal	2.4		N/P
Case 4	25	F	Left parotid	3.1	No LN mets	N/P
Case 5	41	F	Right parotid	1.0	No LVI No PNI No LN mets	N/P
Case 6	74	F	Left parotid	1.8	LVI + PNI + necrosis	N/P
Case 7	68	M	Left parotid	2.5	No LVI No PNI	N/P
Case 8	77	F	parapharyngeal	biopsy	No LVI No PNI	N/P
AciCC-IDC						
Case 1	77	M	Right parotid	3.5	No LN mets	Negative
Case 2	46	M	Left parotid	1.5	No LVI No PNI	Negative
Case 3	22	M	Right parotid	1.4		Negative
Case 4	72	F	Left parotid	3.5	No LVI No PNI	Negative

MASC mammary analog secretory carcinoma, *AciCC* acinic cell carcinoma, *AciCC-IDC* acinic cell carcinoma intercalated duct cell-predominant variant, *yr* year, *cm* centimeters, *M* male, *F* female, *LVI* lymphovascular invasion, *PNI* perineural invasion, *LN mets* lymph node metastasis, *N/P* not performed

integrates composite features from striated ducts cells [14]. The second cell-type, often intertwined with the first cell-type, reveals a dilated endoplasmic reticulum with multiple mitochondria dispersed throughout the cytoplasm (Fig. 1d). These features are suggestive of intercalated duct cell differentiation [14]. It is important to mention that features of both intercalated and striated duct cell differentiation can be found within the same cell (Fig. 1d). Rare scattered cells with medium-to-large intracytoplasmic electron-dense and electron-light zymogen-like granules are identified in only

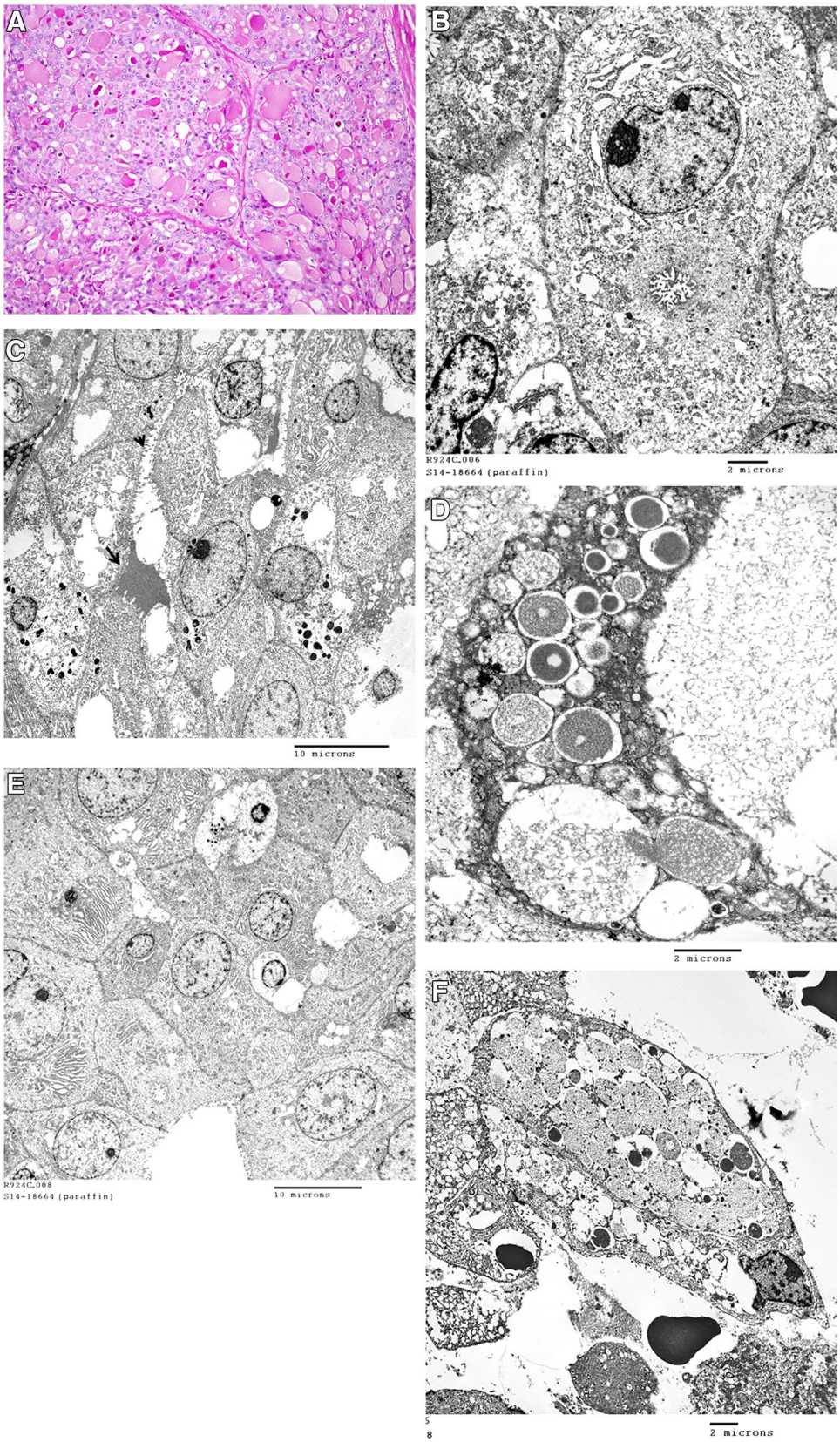

Fig. 1 Mammary analogue secretory carcinoma (MASC). Classic microcystic/cribriform pattern with extracellular eosinophilic secretory material (**a**, H&E, 200X). Electron micrographs with intracellular lumen studded with numerous microvilli (**b**), and flattened to cuboidal cells with intracellular lumens lined with small microvilli (*arrow head*, **c**). These features are suggestive of striated duct cell differentiation. Electron-dense extracellular secretory material is observed (*arrow*). Some cells containing electron-dense secretory/zymogen-like granules are visible (acinar cell differentiation, **c**). Higher powered EM image (**d**) of a cell containing multiple, variably sized secretory vacuoles. Exocytosis of secretory vacuoles is visible (*bottom*). Some cells (**e**) reveal dilated and prominent endoplasmic reticulum with scattered mitochondria, features of intercalated duct cell differentiation. Flat to cuboidal cells with inter- and intracellular lumina studded with microvilli are also visible. A cell with medium-to-large (**f**) intracytoplasmic electron-dense and electron-light zymogen granules recapitulating the acinar cell

one case (Fig. 1e). This cell-type is highly suggestive of acinar differentiation [14, 15].

The eight cases of classic AciCC reveal two important cell populations. The dominant cell population consists of clusters of polygonal cells with medium-to-large intracytoplasmic electron-dense and electron-light zymogen granules, some with prominent endoplasmic reticulum, altogether features of acinar cell differentiation (Fig. 2a). Few of these cells have, in addition to zymogen-like granules, apical cell surface studded with microvilli but no

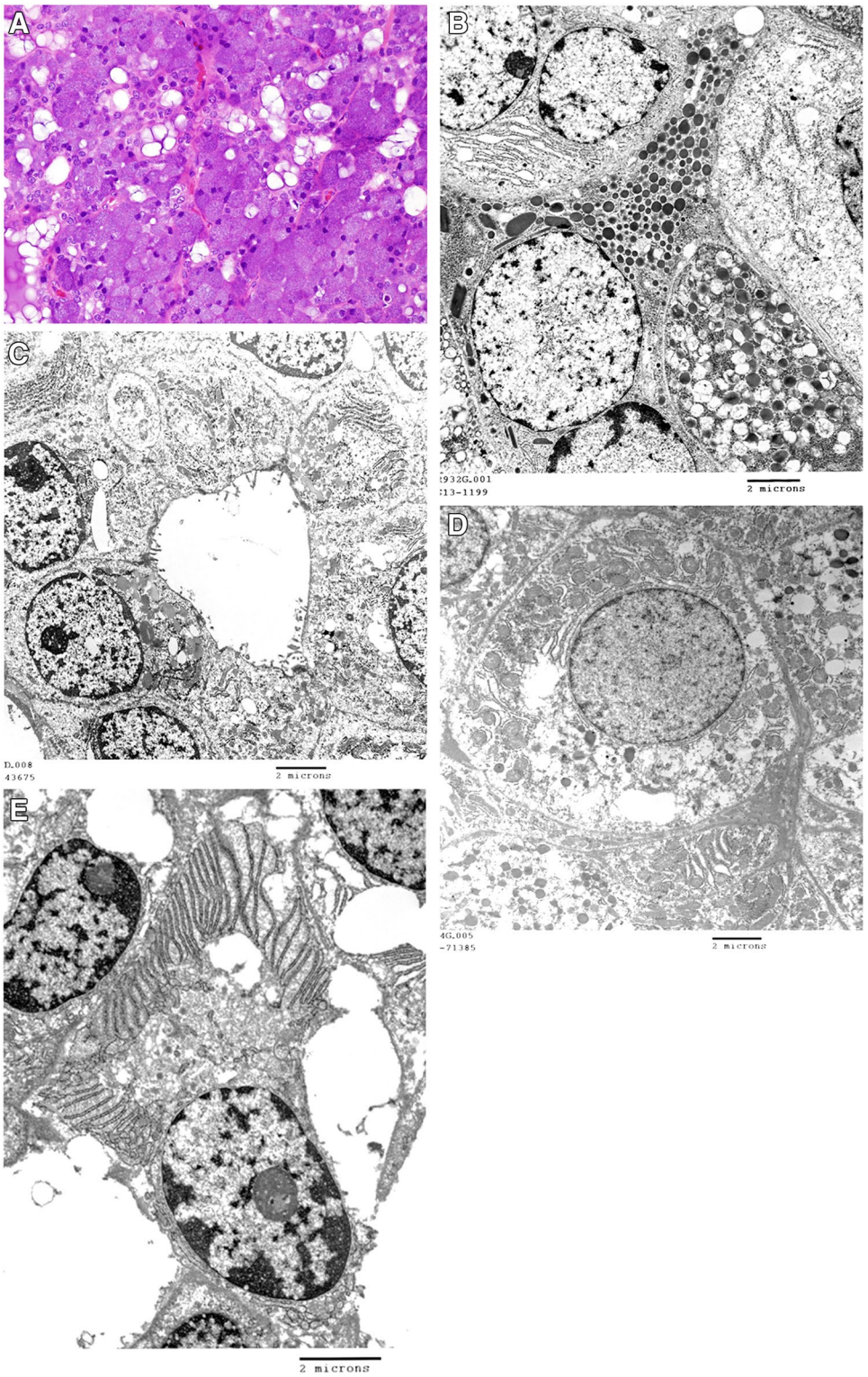

Fig. 2 Acinic cell carcinoma, classical type (AciCC). Microcystic pattern composed of uniform acinar (serous) cells with basophilic granular cytoplasm (**a**, H&E, 400X). Electron micrographs: Cells containing numerous small-to-medium sized electron dense and electron-light zymogen granules in favor of acinar cell differentiation (**b**). Cuboidal cells arranged in a cystic pattern, some with intracytoplasmic electron-dense, zymogen-like granules and with the luminal surface studded by microvilli (**c**). Cell with abundant large mitochondria (**d**), with noted dilated endoplasmic reticulum adjacent to nucleus. Dilated and prominent endoplasmic reticulum (**e**) with small, visible organelles (*center*), likely mitochondria. Features of 2 C and 2D highly suggestive of intercalated duct origin

intracellular lumen is visible (Fig. 2b). The latter can easily be mistaken for striated duct cell differentiation, as reported earlier in MASC. However, apical microvilli may be observed in acinar cell differentiation [14]. Intertwined in these clusters is found a second cell population, which consists of cells with abundant mitochondria and dilated endoplasmic reticulum (Fig. 2c, d). This second cell-type is very similar to those previously observed in MASC, representing intercalated duct cell differentiation [14, 15].

Lastly, AciCC intercalated duct cell-predominant variant reveals combined ultrastructural features of both MASC and classic AciCC. Readily distinguishable intercalated/striated duct cell-types, lacking intracellular lumen or zymogen-like granules, are the dominant cell populations and correspond to the microcystic pattern seen in this tumor (Fig. 3a, b). Cells with acinar differentiation are also visible. Unlike those seen in classic AciCC (Fig. 3c), these cells are fewer in numbers, disperse throughout the tumor, and contain a lesser amount of zymogen-like granules.

Discussion

MASC is a recently described malignancy of salivary glands with a characteristic immunophenotypic and cytogenetic profile. Until this unique ancillary profile was reported, MASC was previously considered to be an AciCC, either "zymogen poor" or intercalated duct cell-predominant variant [5–8, 12, 13]. Although immunohistochemistry and cytogenetic features are very useful for day-to-day diagnosis of MASC, ultrastructural analysis provides additional information on cellular differentiation and on the relationship between MASC, classic AciCC, AciCC intercalated duct cell-predominant variant.

Our study demonstrates that MASC presents distinctive ultrastructural features that allow its proper differentiation from classic AciCC. MASC main cell-type consists of cells with striated/intercalated duct cell differentiation, whereas, classic AciCC dominant cell-type recapitulates acinar cell differentiation [14, 15]. Interestingly, AciCC intercalated duct cell-predominant variant displays significant ultrastructural overlap with both MASC and classic AciCC, as it contained both of their main cell-types. MASC's primary cell-type, striated/intercalated duct cell differentiation, comprises the largest proportion.

MASC, classic AciCC, and AciCC intercalated duct cell-predominant variant are composed of cells that demonstrate composite features common to acinar, intercalated duct, and striated duct cells. Morphologically, acinic cell carcinomas are predominantly composed of acinar cells rich in diastase-resistant zymogen granules. These tumors, with sheets of predominantly acinar cells, are classically recognized as acinic cell carcinoma. When non-granule-rich cells predominate or are at least prominent, other tumor considerations are made. This cell non-granule-rich population defines intercalated duct-cell predominant AciCC, and this variant, especially in microcystic cases, has the most overlap with MASC [15, 16]. Whether these salivary gland tumors originate from or differentiate into these cell-types remain not well understood [17]. Nonetheless, significant histological overlaps are found among these three entities, which suggest a very close proximity between these tumors. A possible interpretation is that MASC and classic AciCC are not entirely separate entities but integrates a spectrum with AciCC intercalated duct cell-predominant variant being an intermediate between the two. An alternative and maybe more pleasing explanation is that AciCC intercalated duct cell-predominant variant may be a peculiar variant rather than a separate entity from MASC or a 'negative translocation' MASC. These hypotheses are supported by the idea that these are low grade tumors sharing a very similar clinicopathological profile and good prognosis [3, 7, 10, 12, 13, 18].

In addition, a series of 19 cases of MASC showed the presence of a translocation (12; 15) (q13; q25) in 18/19 cases, resulting in an *ETV6-NTRK3* gene rearrangement [5]. Of these, a single case of MASC is negative for *ETV6* rearrangement, although an intact *NTRK3* gene was not independently studied in this case. In this particular case, the diagnosis of MASC was based on combined morphologic and immunophenotypic features, supported by a strong and diffuse staining for mammaglobin and S100. On the other hand, cases of AciCC, mimicking MASC, with mammaglobin and/or S100 positivity and a negative translocation have been observed [8], even though these remain rare. If we accept that certain cases of MASC and AciCC, especially the intercalated duct cell-predominant variant, may share an overlapping morphology, a similar staining pattern and a negative translocation, then we can assume that the boundaries between these two entities may not be well-defined.

Nonetheless, additional studies on ultrastructural characterization of MASC and AciCC intercalated duct cell-predominant variant are needed to understand their converging histogenesis. At the time being, the latter should be approached as a 'rule out' MASC and appropriate immunophenotypic, cytogenetic, and EM studies should be performed to provide the correct diagnosis.

As tumor morphology, both microscopic and ultrastructural, belies the unique genetic changes, further studies are needed to elucidate the cellular origin and differentiation of MASC. As more cases are reported, actual outcomes data combined with understanding of divergent tumor genetics may provide insight into tumorigenesis and unique therapeutic modalities [2].

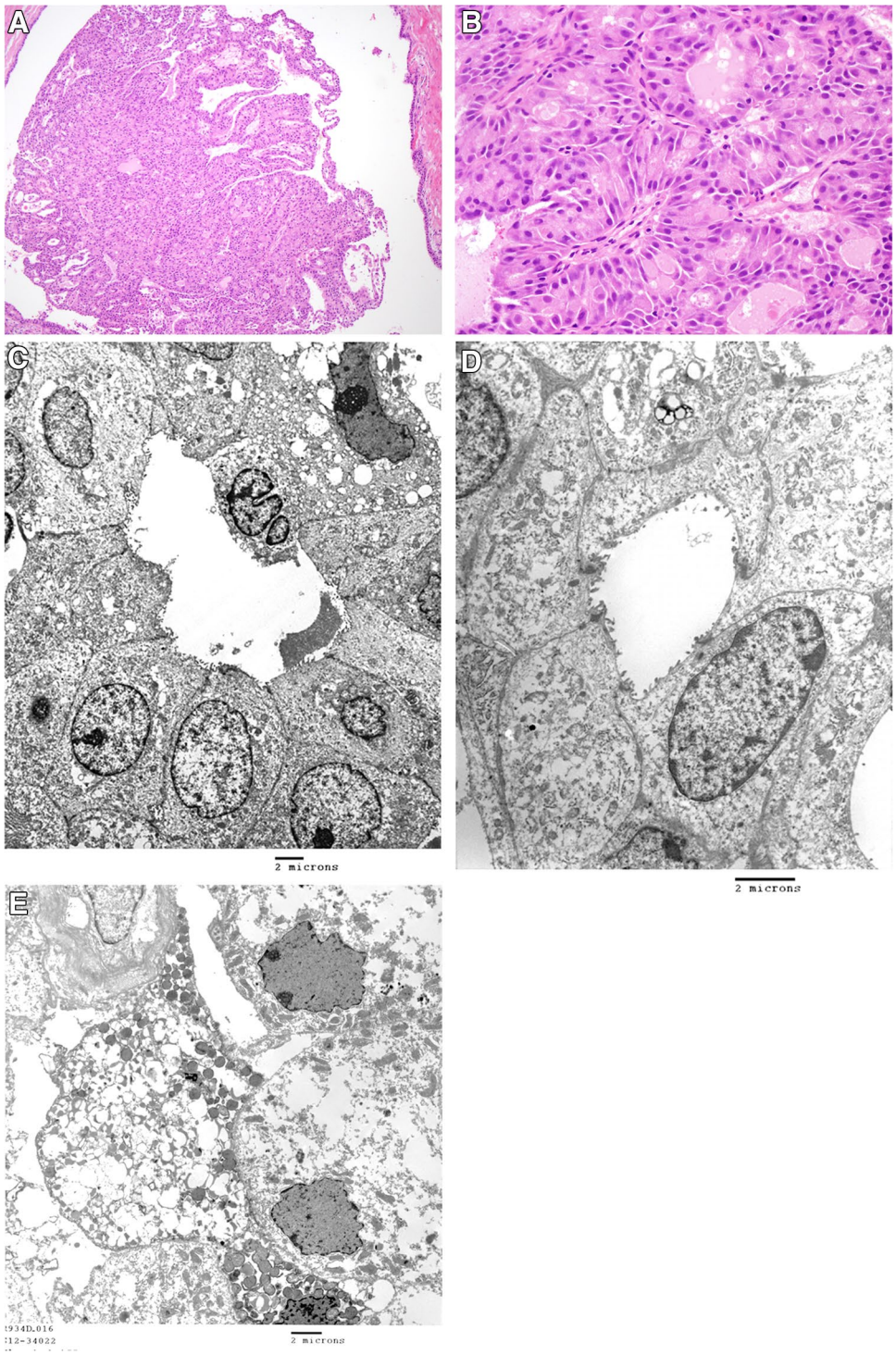

Fig. 3 Acinic cell carcinoma, intercalated duct cell-predominant variant (AciCC IDP). Microcystic and papillary patterns composed of uniform cells with pale cytoplasm and no zymogen granules (H&E; **a**, 100X, **b**, 400X). Electron micrographs: Cuboidal cells arranged in around a central lumen featuring apical surfaces lined by small microvilli and an absence of zymogen or electron dense secretory granules (**c, d**). Scattered cells containing small amounts of electron-dense zymogen-like granules recapitulating acinar cell differentiation (**e**)

Funding The studies are funded by departmental funds available to Dr. Sadow and colleagues, This manuscript was funded by intradepartmental funding at Massachusetts General Hospital.

Compliance with Ethical Standards

Conflict of interest All authors declare that they have no conflict of interest.

Ethical Approval This article does not contain ay studies with human participants performed by the authors.

IRB Approval This Project was approved by the Massachusetts General Hospital Internal Review Board (Sadow, PI; 2015P001749).

References

1. Skálová A, Vanecek T, Sima R, Laco J, Weinreb I, Perez-Ordonez B, Starek I, Geierova M, Simpson RH, Passador-Santos F, Ryska A, Leivo I, Kinkor Z, Michal M. Mammary analogue secretory carcinoma of salivary glands, containing the ETV6-NTRK3 fusion gene: a hitherto undescribed salivary gland tumor entity. Am J Surg Pathol. 2010;34(5):599–608.
2. Drilon A, Li G, Dogan S, Gounder M, Shen R, Arcila M, Wang L, Hyman DM, Hechtman J, Wei G, Cam NR, Christiansen J, Luo D, Maneval EC, Bauer T, Patel M, Liu SV, Ou SH, Farago A, Shaw A, Shoemaker RF, Lim J, Hornby Z, Multani P, Ladanyi M, Berger M, Katabi N, Ghossein R, Ho AL. What hides behind the MASC: clinical response and acquired resistance to entrectinib after ETV6-NTRK3 identification in a mammary analogue secretory carcinoma (MASC). Ann Oncol. 2016;27(5):920–6.
3. Luk PP, Selinger CI, Eviston TJ, Lum T, Yu B, O'Toole SA, Clark JR, Gupta R. Mammary analogue secretory carcinoma: an evaluation of its clinicopathological and genetic characteristics. Pathology. 2015;47(7):659–66.
4. Skálová A, Vanecek T, Simpson RH, Laco J, Majewska H, Baneckova M, Steiner P, Michal M. Mammary Analogue Secretory Carcinoma of Salivary Glands: Molecular Analysis of 25 ETV6 Gene Rearranged Tumors With Lack of Detection of Classical ETV6-NTRK3 Fusion. Transcript by Standard RT-PCR: Report of 4 Cases Harboring ETV6-X Gene Fusion. Am J Surg Pathol. 2016;40(1):3–13.
5. Shah AA, Wenig BM, LeGallo RD, Mills SE, Stelow EB. Morphology in conjunction with immunohistochemistry is sufficient for the diagnosis of mammary analogue secretory carcinoma. Head Neck Pathol. 2015;9(1):85–95.
6. Patel KR, Solomon IH, El-Mofty SK, Lewis JS Jr, Chernock RD. Mammaglobin and S-100 immunoreactivity in salivary gland carcinomas other than mammary analogue secretory carcinoma. Hum Pathol. 2013;44(11):2501–8.
7. Skalova A. Mammary analogue secretory carcinoma of salivary gland origin: an update and expanded morphologic and immunohistochemical spectrum of recently described entity. Head Neck Pathol. 2013;7(Suppl 1):S30–6.
8. Pinto A, Nosé V, Rojas C, Fan YS, Gomez-Fernandez C. Searching for mammary analogue [corrected] secretory carcinoma of salivary gland among its mimics. Mod Pathol. 2014;27(1):30–7.
9. Bishop JA. Unmasking MASC: bringing to light the unique morphologic, immunohistochemical and genetic features of the newly recognized mammary analogue secretory carcinoma of salivary glands. Head Neck Pathol. 2013;7(1):35–9.
10. Chiosea SI, Griffith C, Assaad A, Seethala RR. Clinicopathological characterization of mammary analogue secretory carcinoma of salivary glands. Histopathology. 2012;61(3):387–94.
11. Ito Y, Ishibashi K, Masaki A, Fujii K, Fujiyoshi Y, Hattori H, Kawakita D, Matsumoto M, Miyabe S, Shimozato K, Nagao T, Inagaki H. Mammary analogue secretory carcinoma of salivary glands: a clinicopathologic and molecular study including 2 cases harboring ETV6-X fusion. Am J Surg Pathol. 2015;39(5):602–10.
12. Urano M, Nagao T, Miyabe S, Ishibashi K, Higuchi K, Kuroda M. Characterization of mammary analogue secretory carcinoma of the salivary gland: discrimination from its mimics by the presence of the ETV6-NTRK3 translocation and novel surrogate markers. Hum Pathol. 2015;46(1):94–103.
13. Griffith C, Seethala R, Chiosea SI. Mammary analogue secretory carcinoma: a new twist to the diagnostic dilemma of zymogen granule poor acinic cell carcinoma. Virchows Arch. 2011;459(1):117–8.
14. Resta L, Piscitelli D, Fiore MG, Sanguedolce F. Role of electron microscopy in diagnosis of parotid tumours. Acta Otorhinolaryngol Ital. 2005;25(3):150–2.
15. Dardick I, George D, Jeans MT, Wittkuhn JF, Skimming L, Rippstein P, van Nostrand AW. Ultrastructural morphology and cellular differentiation in acinic cell carcinoma. Oral Surg Oral Med Oral Pathol. 1987;63(3):325–34.
16. Lei Y, Chiosea SI. Re-evaluating historic cohort of salivary acinic cell carcinoma with new diagnostic tools. Head Neck Pathol. 2012;6(2):166–70.
17. Chaudhry AP, Cutler LS, Leifer C, Labay G, Satchidanand S, Yamane GM. Ultrastructural study of the histogenesis of salivary gland mucoepidermoid carcinoma. J Oral Pathol Med. 1989;18(7):400–9.
18. Chiosea SI, Griffith C, Assaad A, Seethala RR. The profile of acinic cell carcinoma after recognition of mammary analog secretory carcinoma. Am J Surg Pathol. 2012;36(3):343–50.